J Electroceram (2007) 19:333–338
DOI 10.1007/s10832-007-9055-0

Screen-printed piezoceramic thick films for miniaturised devices

R. Lou-Moeller · C. C. Hindrichsen · L. H. Thamdrup · T. Bove · E. Ringgaard · A. F. Pedersen · E. V. Thomsen

Received: 3 March 2006 / Accepted: 21 August 2006 / Published online: 8 March 2007

Abstract The development towards smaller devices with more functions integrated calls for new and improved manufacturing processes. The screen-printing process is quite well suited for miniaturised and integrated devices, since thick films can be produced in this manner without the need for further machining. On the other hand, the process of screen printing thick films involves potential problems of thermal matching and chemical compatibility at the processing temperatures between the functional film, the substrate and the electrodes. As an example of such a miniaturised device, a MEMS accelerometer based on PZT thick film will be presented. The design and process flow of this accelerometer has been optimised by means of finite element modelling (FEMLAB©). Consequently it has proved possible to eliminate post-processing steps after the screen printing of the PZT thick film.

Keywords Thick-film · Piezoceramic · MEMS · PZT

1 Introduction

In state-of-the-art production, piezoelectric parts are manufactured as discrete elements, machined from bulk ceramic to specific dimensions and assembled with other components at the end of the production line. This top-down approach imposes limits to the minimum dimension of the parts manufactured and it constrains the geometry of the parts to simple shapes like discs, plates, rings, cylinders etc. The bottom–up approach of thin film technology is limited by a maximum dimension of about 1 μm. Consequently, there is a gap between the bulk technology and the thin film technology spanning 1–100 μm. One of the candidates for filling a part of this gap is the technology of screen printed PZT thick film (*TF*) [1, 2]. The technology of thick film is well established in the industry and the implementation of an extra element in the form of piezoelectric films is a natural development. This implementation requires investigation of piezoelectric materials compatible with thick film technology and the substrates, which could be considered in various applications. The most crucial issue of compatibility between piezoelectric materials and interesting substrates is the temperature at which the ceramic is sintered. Consequently, one of the challenges in the development of this technology has been to reduce the sintering temperature. The solution to this problem is the introduction of a sintering aid, which assists densification of the film at temperatures as low as 800–900°C [3, 4]. Another challenge is the functional characterisation of the thick film. The substrate will inevitably influence the measurement and the manner in which the properties of the film are extracted from the measurement should be considered carefully.

R. Lou-Moeller (✉) · E. Ringgaard
Ferroperm Piezoceramics A/S,
Kvistgaard, Denmark
e-mail: rm@ferroperm-piezo.com

C. C. Hindrichsen · L. H. Thamdrup · E. V. Thomsen
Department of Micro and Nanotechnology (MIC), Technical University of Denmark (DTU),
Kgs. Lyngby, Denmark

T. Bove · A. F. Pedersen
InSensor A/S,
Kvistgaard, Denmark

2 Sample preparation

The substrates used in this study were silicon, alumina and porous PZT ceramic, and have been selected on the basis of potential applications. Silicon is interesting because of applications in microelectromechanical systems (MEMS).

Alumina is a relatively inert material, widely used as a substrate in the electronics industry, well known and affordable. TF on porous PZT has applications for high frequency transducers due to the low acoustic impedance of the substrate.

The PZT paste used for the printing of the films was made out of a commercially available composition, TF2100 from Insensor A/S which is a Ferroperm Pz26 (NAVY type 1) composition, with a sintering aid. The PZT powder is ball milled to a mean particle size of about 1 μm. The milled powder is then suspended in an organic vehicle and homogenised in a triple roller mill forming a printable paste.

The thickness of the alumina and the porous PZT substrates was 1 mm, whereas the silicon substrate thickness was 500 μm. In the case of alumina and porous PZT, a gold bottom electrode was printed directly on the substrate. In the case of the silicon substrate, the chemical incompatibility between PZT and silicon has made it necessary to introduce a platinum layer deposited by a conventional sputtering technique (see for instance [5]). The Pt layer acts as a barrier between the substrate and the PZT. After deposition of the bottom electrode, up to eight layers of PZT were printed and subsequently sintered at 850°C for 1 h in a chamber furnace, giving a film thickness of about 50 μm. The thickness was measured using a micrometer and verified later in the SEM pictures of the cross-section of the film. A silver top electrode was deposited by screen printing and fired separately in a conveyer belt furnace with a peak temperature of 700°C (Figs. 1 and 2).

Due to the intrinsic porosity of the film, the electrical properties are highly sensitive to moisture in the atmosphere. This sensitivity was eliminated by submerging the sample into a mineral oil, heated to a temperature of 150°C. The action of the oil is to extract the water and seal off the pores. After the oil treatment, the sample is poled at 150°C in air with an applied field of 10 kV/mm for 10 min. After this, microstructural and electrical characterisation was performed.

3 Characterisation

In order to evaluate the quality of the TF, SEM microscopy, measurements of the relative permittivity and hysteresis loops were performed.

Fig. 1 A cross-sectional view of the entire structure. The barrier layer is only necessary when a silicon substrate is used

Fig. 2 A picture of the actual structure taken with a digital camera. Alumina substrate on the *left* and silicon substrate on the *right*. Each sample is 30×30 mm^2

As seen from the SEM pictures a general feature of the PZT film is a certain degree of porosity arising from the sintering conditions (Fig. 3). As the densification of the film is not caused by grains merging, but rather by capillary forces from the liquid phase sintering aid, there is very limited grain growth. The grain size is therefore more or less conserved during sintering, giving the film a very characteristic microstructure, which is different from bulk ceramic densified at high temperature. The densification is also affected by mechanical clamping from the substrate.

In the case of porous PZT, the roughness of the substrate is comparable to the thickness of the TF. Therefore, a few layers of PZT are printed before the bottom electrode, which is seen to reduce the roughness of the substrate to a minimum.

Figure 4 depicts the relative permittivity as a function of temperature. A pellet of Pz26 without sintering aid densified at high temperature is included as a reference. When comparing the films and bulk Pz26, the only difference is a scaling factor, depending on substrate. The reduction of the permittivity is a consequence of several factors. Firstly, it has been argued elsewhere that the sintering aid forms a low permittivity phase at the grain boundary [6] decreasing the mean permittivity of the entire film. Also, the inherent porosity of the TF contributes. The film could be viewed as a composite of a ceramic with spherical inclusions, or pores [7]. A quantitative evaluation of the contribution from this is not given here, but it is considered to be the preponderant factor. The last contribution to the lowering of the permittivity arises from the mechanical clamping from the substrate. This effect is however difficult to evaluate as the free permittivity of the film has not been determined.

For verification of ferroelectric behaviour, measurements of hysteresis were performed using a Sawyer–Tower setup (Fig. 5). The electrical field was applied as a single period of a sawtooth waveform with a frequency of 50 Hz. All films exhibit typical ferroelectric hysteresis. Compared to

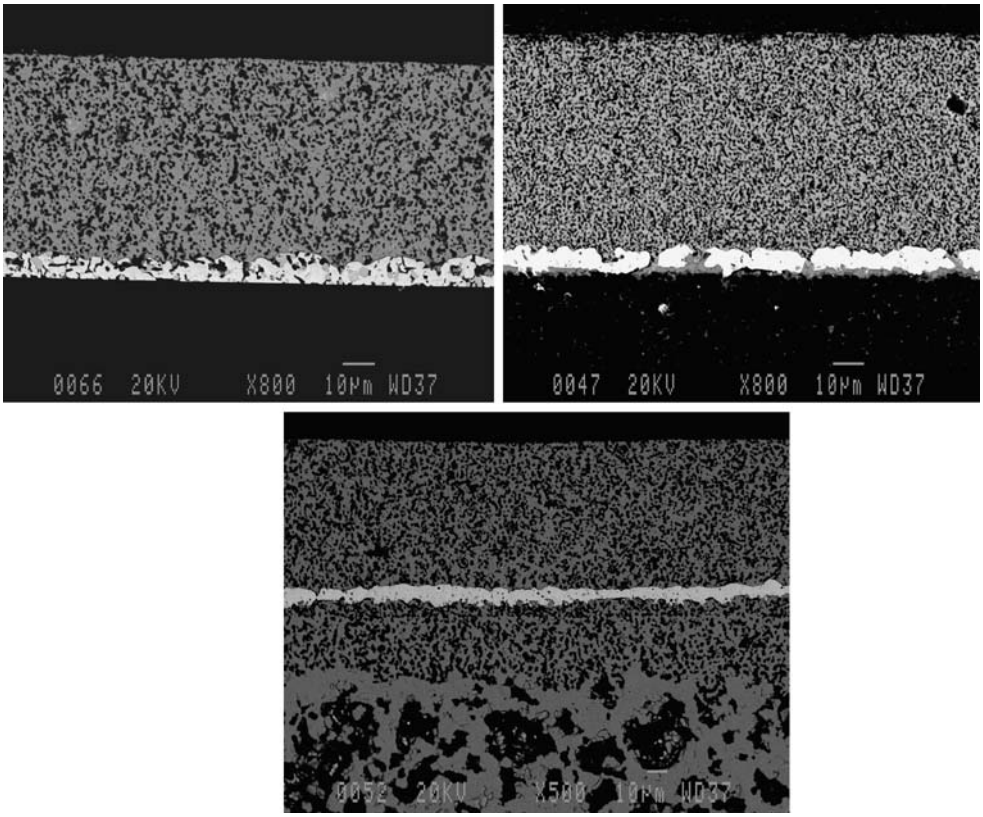

Fig. 3 SEM image of a cross section of a PZT thick film on a silicon substrate (*upper left*), alumina substrate (*upper right*) and porous PZT substrate (*lower*). The extra PZT layer on the porous substrate is easily discerned

the Pz26 pellet, the films exhibit a deterioration of remnant polarisation. This deterioration emanates from the same factors causing the reduction of permittivity, i.e. the presence of a low-permittivity dielectric phase and porosity. An additional effect is the mechanical clamping, which may affect the dipole alignment. This effect is known from thin film, but the quantitative evaluation in the case of thick films falls outside the scope of this paper.

As an evaluation of the performance of the TF, a measurement of the strain of the thick film as a function

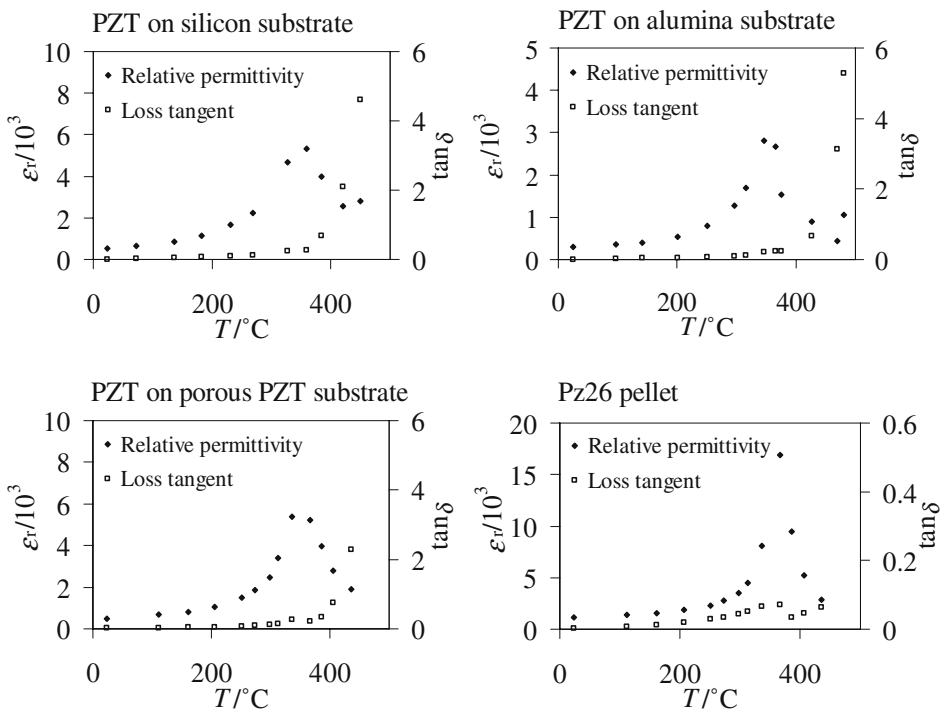

Fig. 4 Relative permittivity of the TF as a function of temperature

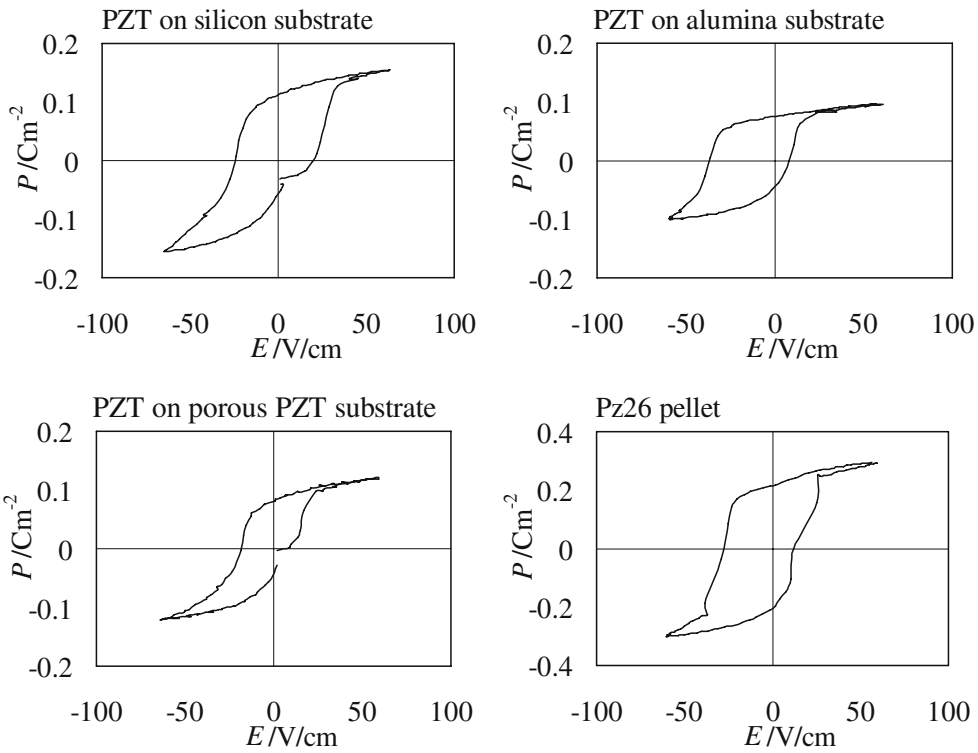

Fig. 5 Measurements of hysteresis loops performed, using a Sawyer–Tower setup. In comparison with bulk Pz26, a deterioration of remnant polarization is observed in all films

of applied electric field was performed (Fig. 6). The equipment used was a fiber-optic probe system developed at Ecole Polytechnique Fédérale de Lausanne (EPFL), Laboratoire de Céramique.

The displacement of the surface is related to the d_{33} coefficient in the film, but the result of the measurement cannot be translated into a measurement of the actual d_{33} coefficient of the material. Due to the clamping from the substrate, the measured coefficient is reduced by a contribution from the d_{31} coefficient. The resulting apparent d_{33} coefficient will here be referred to as $d_{33,f}$ [8]. Another contribution caused by the d_{31} coefficient is the bending of

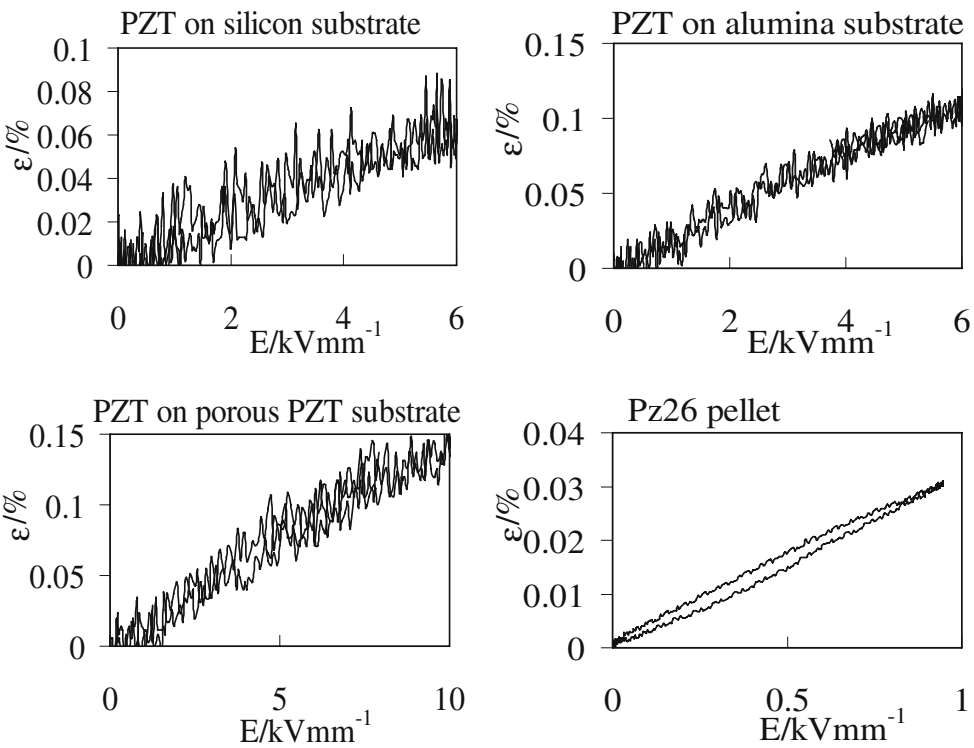

Fig. 6 Measurement of the displacement of the thick film surface as a function of applied voltage

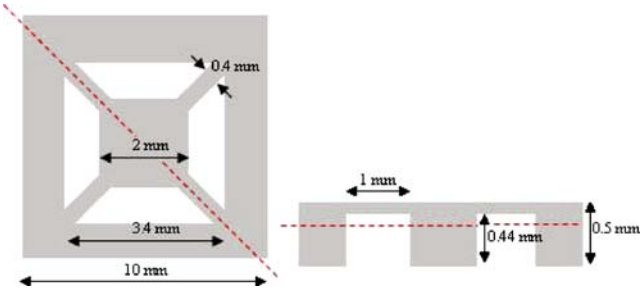

Fig. 7 Dimensions of the accelerometer design as seen from above (*left*) and the cross-section (*right*)

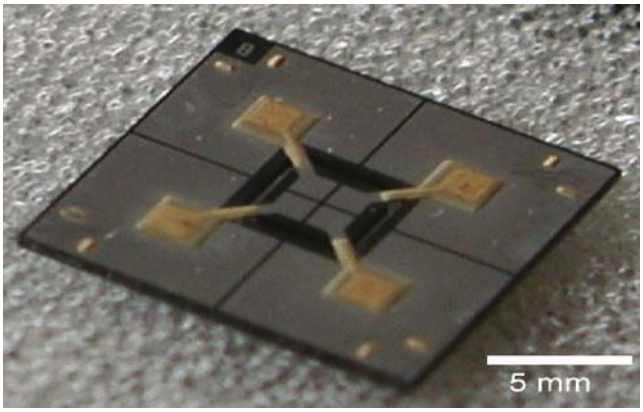

Fig. 9 Optical image of the actual device

the entire structure [9]. This bending was eliminated by fixing the substrate to a thick slab of ceramic alumina using high-strength cement. The apparent $d_{33,f}$ is calculated by linear regression and the results are 110, 180 and 145 pm/V for films on silicon, alumina and porous PZT, respectively. For comparison, a measurement of a pellet of bulk Pz26 is included for which the actual d_{33} coefficient calculated from this measurement is 310 pm/V. Since the $d_{33,f}$ has a contribution from d_{31} depending on substrate properties it is not directly comparable between films on different substrates. For a complete picture of the functionality of the film, a measurement of d_{31} is necessary and this work is under way.

Nevertheless, the simple displacement measurement has significance as it is directly related to the activity of the film.

4 MEMS accelerometer

As an example of a functional device utilizing PZT TF a MEMS accelerometer was developed in collaboration with the Department of Micro and Nanotechnology (MIC) at the Technical University of Denmark (DTU). The accelerometer consists of a central seismic mass of 4.7×10^{-6} kg, supported by four diagonally oriented cantilevers as seen in Fig. 7. The design was partly adapted from [10]. 3D finite element modelling, using FemLab©, was performed in order to determine the optimal position of the active PZT TF (Fig. 8). To maximize the output signal, it is vital that the active PZT layer does not extend all the way out to the seismic mass. As evident from Fig. 8, there is a negative stress contribution in close vicinity to the seismic mass.

The clean room process flow has been developed, aiming to eliminate post processing after the PZT TF deposition. 500 μm thick double-side polished 4" (100) silicon wafers were used as substrates. The process flow consists of an advanced silicon etch (ASE) process thinning down the cantilevers, a wet thermal oxidation used for insulating the individual electrodes, an electron beam deposition of the dedicated barrier and bottom electrode layers and an ASE process used for releasing the seismic mass and cantilevers.

Fig. 8 FemLab simulation indicating the stress distribution in the PZT TF (*top layer*) and the cantilever caused by a displacement between the seismic mass and the frame

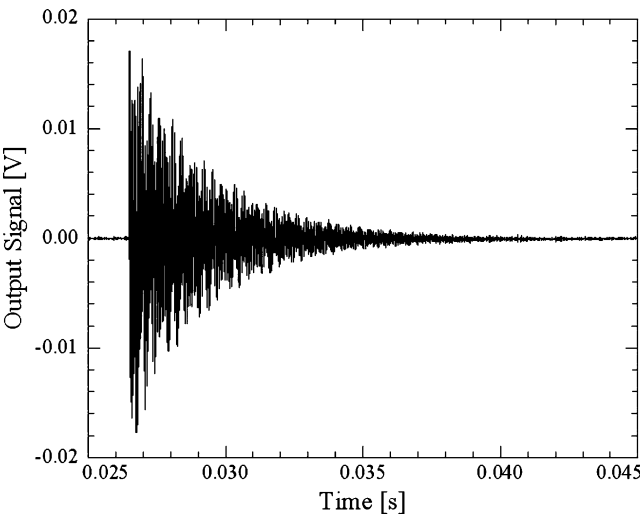

Fig. 10 Representative example of the output voltage as a function of time after an impact. The cantilevers supporting the seismic mass were not thinned down on this accelerometer

Conventional positive photo-resist was used as masking material in both ASE processes. Following the clean room work, approximately 50 μm PZT and a top electrode (5 μm Au) was screen printed at Insensor A/S. It proved possible to successfully screen print on cantilevers with thicknesses down to 60 μm. An image of the final device can be seen in Fig. 9.

Before performing test of the device, top and bottom electrodes were wire bonded to a printed circuit board. The functionality of the MEMS device was verified by measuring the output voltage after a single high acceleration impact event. A PCI card (National Instruments PCI-4474) with a sample rate of 100 kHz was used for data acquisition. As expected, the output voltage resembles that of an exponentially decaying oscillation (Fig. 10).

Presently work is carried out in order to establish a more thorough characterisation of accelerometers utilizing PZT TF as the sensor material.

5 Conclusion

Characterisation of PZT TF sintered at temperatures compatible to materials used in the electronics, hybrid circuit and silicon industry has been reported. As expected, the performance is lower compared to bulk ceramics sintered under free conditions at high temperature due to the microstructure and the clamping of the substrate. However, with all these conditions working against the film, the activity, based on the measurement of the apparent d_{33} is still significant.

An example of a MEMS accelerometer, merging the powerful and versatile technology of silicon micromachining and PZT thick film, has been presented. The output signal from an impact event was measured, verifying the functionality of the device and the PZT film.

Acknowledgements D. Damjanovic and co-workers from EPFL for help with d_{33} and ferroelectric hysteresis measurements and Barbara Malic and co-workers at the Jozef Stefan Institute for help with SEM microscopy.

Part of this work is supported by the EC through the MINUET project (6th Framework Programme, Contract no. NMP2-CT-2004-505657).

References

1. N.M. White, J.D. Turner, Meas. Sci. Technol. **8**, 1–20 (1997)
2. W.W. Wolny, 12th IEEE ISAF proceedings, 257–262 (2000)
3. D.L. Corker, R.W. Whatmore, E. Ringgaard, W.W. Wolny, J. Eur. Ceram. Soc. **20**, 2039–2045 (2000)
4. P. Tran-Huu-Hue, F. Levassort, F.V. Meulen, J. Holc, M. Kosec, M. Letheicq, J. Eur. Ceram. Soc. **21**, 1445–1449 (2001)
5. F. Akasheh, T. Myers, J.D. Fraser, S. Bose, A. Bandyopadhyay, Sens. Actuators, A **111**, 275–287 (2003)
6. F.F.C. Duval, R.A. Dorey, Q. Zhang, R.W. Whatmore, J. Eur. Ceram. Soc. **23**, 1935–1941 (2003)
7. D.J. Bergman, Phys. Rep. **43**, 377–407 (1978)
8. R.N. Torah, S.P. Beeby, N.M White, J. Phys. D: Appl. Phys. **37**, 1074–1078 (2004)
9. A. Berzegar, D. Damjanovic, N. Ledermann, P. Muralt, J. Appl. Physi. **93**, 4756–4760 (2003)
10. S.P. Beeby, J.N. Ross, N.M. White, J. Micromechanics Microengineering **10**, 322–328 (2000)